Comprehensive analysis of differential gene expression profiles on D-galactosamine-induced acute mouse liver injury and regeneration

Heekyoung Chung [a,b], Hyun-Jun Kim [a], Ki-Seok Jang [a], Mingoo Kim [c], Jungeun Yang [d],
Kyung-Sun Kang [b,e], Hyung-Lae Kim [b,f], Byung-Il Yoon [b,g], Mi-Ock Lee [b,h],
Byung-Hoon Lee [b,i], Ju Han Kim [b,c], Yong-Sung Lee [d], Gu Kong [a,b,*]

[a] *Department of Pathology, College of Medicine, Hanyang University, 17 Haengdang-dong, Seongdong-gu, Seoul 133-791, Republic of Korea*
[b] *Toxicogenomics Research Consortium (TGRC), Hanyang University, Seoul 133-791, Republic of Korea*
[c] *Seoul National University Biomedical Informatics (SNUBI), Seoul National University College of Medicine, Seoul 110-799, Republic of Korea*
[d] *Department of Biochemistry, College of Medicine, Hanyang University, Seoul 133-791, Republic of Korea*
[e] *Department of Veterinary Public Health, College of Veterinary Medicine, Seoul National University, Seoul 151-742, Republic of Korea*
[f] *Department of Biochemistry, College of Medicine, Ewha Womans University, Seoul 158-710, Republic of Korea*
[g] *School of Veterinary Medicine, Kangwon National University, Chuncheon 200-701, Republic of Korea*
[h] *College of Pharmacy and Bio-MAX Institute, Seoul National University, Seoul 151-742, Republic of Korea*
[i] *College of Pharmacy and Research Institute of Pharmaceutical Sciences, Seoul National University, Seoul 151-742, Republic of Korea*

Abstract

Microarray analysis of RNA from D-galactosamine (GalN)-administered mouse livers was performed to establish a global gene expression profile during injury and regeneration stages at two different doses. A single dose of GalN at 266 or 26.6 mg/kg body weight was given intraperitoneally, and the liver samples were obtained after 6, 24, and 72 h. Histopathologic studies enabled the classification of the D-galactosamine effect into injury (6, 24 h) and regeneration (72 h) stages. By using the Applied Biosystems mouse genome survey microarray, a total of 7267 out of 33,315 (21.8%) genes were found to be statistically reliable at $p < 0.05$ by two-way ANOVA, and 1469 (4.4%) probes at false discovery rate <5% by significance analysis of microarray. Among the statistically reliable clones by both analytical methods, 389 genes were differentially expressed when compared with non-treated control, with more than a 1.625-fold difference (which equals 0.7 in $\log_2$ scale) at one or more GalN treatment conditions and with less than 1.625-fold difference at all three vehicle-treated conditions. Three hundred thirty six genes and 13 genes were identified as injury- and regeneration-specific genes, respectively, showing that most of the transcriptomic changes were seen during the injury stage. Furthermore, multiple genes involved in protein synthesis and degradation, mRNA processing and binding, and cell cycle regulation showed variable transcript levels upon acute GalN administration.
© 2006 Elsevier Ireland Ltd. All rights reserved.

Keywords: D-Galactosamine (GalN); Mouse; Liver; Toxicogenomics; Applied Biosystems mouse genome survey microarray

1. Introduction

D-Galactosamine (GalN) is a hepatotoxin frequently used to induce experimental liver injury (Keppler et al., 1968). Excessive doses of GalN induce fatal liver injury, which histologically resemble human fulminant hepatic

failure, while transient acute liver injury is observed at lower doses (Keppler et al., 1968). High dose of GalN is known to cause hepatic necrosis by UTP depletion, leading to inhibition of RNA synthesis (Plaa, 1991) and induction of apoptosis of the liver in rat and mice, which is evidenced by histochemical observations, DNA laddering, or caspase-3 activation (Tsutsui et al., 1997; Muntane et al., 1998; Sun et al., 2003). Few genes are reported to play roles in the GalN-mediated hepatic injury and regeneration. Tumor necrosis factor-α is known to mediate GalN-induced cell death, while interleukin-6, hepatocyte growth factor (HGF), transforming growth factor-α are involved in the molecular signaling mediating hepatocyte proliferation during liver regeneration (Fausto, 2000). In addition, HGF, matrix metalloproteinase-13, and tissue inhibitor of proteinase-1 mRNAs are induced during regeneration (Kinoshita et al., 1989; Yata et al., 1999; Lozano et al., 2003). However, global gene changes induced by GalN treatment have not been seen so far, which may be helpful in understanding the molecular mechanism of GalN-mediated hepatic injury and regeneration.

Microarray technology has successfully been applied as a high throughput tool in identifying and characterizing changes in gene expression associated with toxicity, providing informative markers of toxicity, as well as insights on the mechanisms of action (Schena et al., 1995; Nuwaysir et al., 1999).

In the current study, we established an injury-regeneration model of hepatotoxicity by GalN and investigated the global transcriptomic changes during the full chronological stages. Minimal doses of GalN were administered by intraperitoneal (i.p.) injection, which was much lower than the reported doses for the induction of hepatic injury, based on our hypothesis that the highly sensitive microarray technology would enable us to detect transcriptomic changes with a much milder intoxication regimen. We utilized the Mouse Genome Survey Microarray that contains approximately 34,000 60-mer oligonucleotide probes representing 32,381 curated genes that target 44,498 transcripts and nearly 1000 control probes from Applied Biosystems.

2. Materials and methods

2.1. Animal treatment and sample collection

Male ICR mice (Japan SLC; Hamamatsu, Japan) aged 6 weeks were maintained in the specific pathogen-free facility (Hanyang University; Seoul, Republic of Korea) in accordance with the guidelines prepared by the National Academy of Sciences. Animal grouping and treatment regimen were identical

as described (Chung et al., 2006) except that the toxicant was administered by i.p. injection. A total of 50 animals were used initially for sample collection at 5 animals per condition: 5 animals for non-treated and 45 animals for 9 drug-treated conditions [3 different doses (vehicle, low, high) at 3 different time points (6, 24, 72 h)]. Vehicle, low dose, and high dose correspond to 0.1 ml of 0.9% NaCl, 26.6 mg/kg body weight of GalN (Sigma–Aldrich, St. Louis, MO) in 0.1 ml of 0.9% NaCl, and 266 mg/kg body weight of GalN in 0.1 ml of 0.9% NaCl, respectively. High dose used in the present study was based on the results of preliminary studies as the minimal dose that yielded histopathologic hepatotoxicity at 24 h after drug treatment (data not shown). High and low doses correspond to 1/10th and 1/100th of LD50, respectively. The route of administration and the solvent (0.9% NaCl) have been adopted from the report of Hecht et al. (2001). Time points for injury (24 h) and regeneration (72 h) were set as the maximum serum transaminase levels and recovery are seen at 24 h and beyond 48 h, respectively (Hecht et al., 2001). The time point of 6 h was chosen arbitrarily as a time point for early injury. Left lateral lobe of the liver was collected for further analysis.

2.2. Histopathological analysis

The liver tissues from 50 animals were stained with hematoxylin and eosin and examined independently by two pathologists as described (Chung et al., 2005a).

2.3. Serum transferase assays

Serum samples were prepared from blood withdrawn by heart puncture (Isozaki et al., 2002). Serum aspartate aminotransferase (AST) and alanine aminotransferase (ALT) levels of 50 animals were measured as described (Reitman and Frankel, 1957).

2.4. Total RNA isolation

Frozen tissues were pulverized in liquid nitrogen-cooled mortar and pestle apparatus. The powdered tissue was then processed with Trizol (Invitrogen, Carlsbad, CA) for isolation of total RNA, followed by RNeasy (Qiagen, Valencia, CA) purification. Purified total RNAs were analyzed with Agilent 2100 Bioanalyzer (Agilent Technologies, Palo Alto, CA).

2.5. Expression profiling on applied biosystems expression array system

The applied biosystems mouse genome survey microarray contains 33,315 probes, representing 32,381 curated genes targeting 44,498 transcripts. Three animals out of five per each group were selected as representative animals from each group on the basis of biochemical and histopathological review, and total RNA from the selected three animals were further processed. Digoxigenin-UTP labeled cRNA generation, array hybridization (three arrays per treatment condition),

Table 1
Primer sequences used to validate the microarray results by semi-quantitative RT-PCR

Gene	Spot ID	Accession No.	Sense primer	Antisense primer
Cai	330017	NM009787	ataccttcgccattgctgac	caccttgactggtcccttgt
Mist1	751756	NM010800	tggtggctaaagctacgtgtc	gactggggtctgtcaggtgt
G6pc	333144	NM008061	gattccggtgtttgaacgtc	tccaaagtccacaggaggtc
Tieg1	932625	NM013692	agcaagggtcactcctcaga	acatgggacaggcaaacttc
Acacb	778366	AK076301	ccggaagaaagatctggtga	cagtcttccattccagcaca
Igfbp1	694508	NM008341	agcccagagatgacagagga	tctccatccagggatgtctc
8430408G22Rik	632184	NM145980	acagcacatcgtcctgactg	ctgacatttcccgaatcgtt
Dbp	713041	NM016974	accgtggaggtgctaatgac	tggctgcttcattgttcttg
Serpina12	464315	NM026535	acagccacatttgtccttcc	accttcaggcttcgatgaga
Efna1	792870	NM010107	ccctctggcatctcatcact	caaccttggaggcactcttc

chemiluminescence detection, image acquisition and analysis were performed as described (Chung et al., 2006). A total of 30 arrays were run for the RNA samples from 30 animals for 10 experimental conditions (3 biological replicates per condition).

2.6. Microarray data analysis

Assay normalized signals with quality flag <100 were used for the analysis. Filtered values were imputed using KNN imputation algorithm (Troyanskaya et al., 2001). Data were
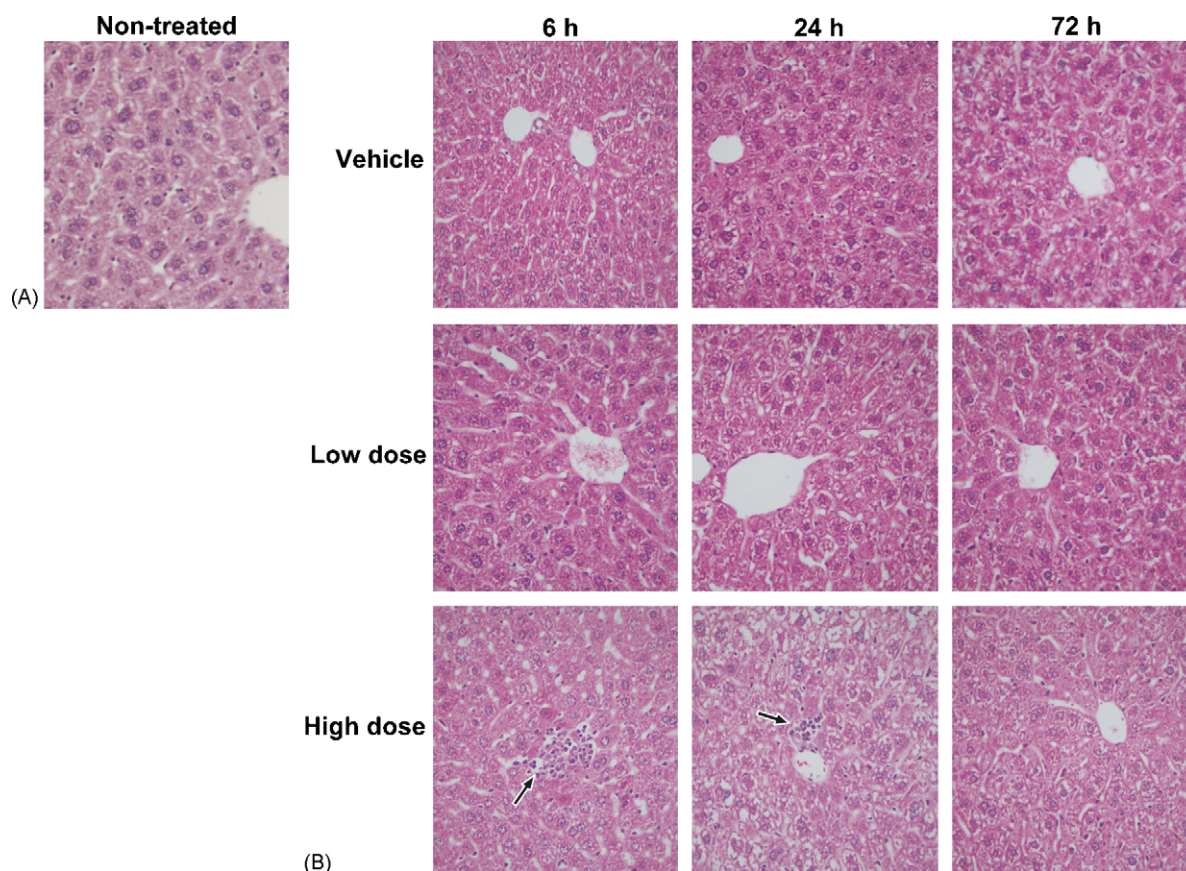

Fig. 1. Sequential histopathologic changes of mouse liver treated with low and high doses of galactosamine (H&E, ×400). (A) Normal histology of non-treated liver. (B) Sections from liver treated with vehicle only showed no histologic changes at all three time points. Sections from liver treated with low dose of galactosamine showed no histologic changes at 0, 24, and 72 h. Sections from liver treated with high dose of galactosamine showed spotty necrosis of hepatocytes with lymphocytic infiltration (arrow) at 6 h, ballooning degeneration and spotty hepatocellular necrosis with lymphocytic infiltration (arrow) at 24 h, and recovery at 72 h.

transformed by variance stabilizing normalization method (Huber et al., 2002) followed by quantile-normalization across array (Bolstad et al., 2003). Two-way ANOVA and significance analysis of microarray (SAM: http://www-stat.stanford.edu/~tibs/SAM) were applied to determine statistically reliable genes. Genes with different dose and time effects were identified and classified into eight groups by two-way ANOVA as described (Chung et al., 2006). SAM was performed using R statistical package (Ihaka and Gentleman, 1996) and default parameters were used when unspecified. Gene ontology (GO) and pathway-based enrichment studies were performed for each cluster (Chung et al., 2004, 2005b). Genes were also subjected to Gene Map Annotator and Pathway Profiler (GenMAPP) analysis (www.genmapp.org), which enables visualization of gene expression by microarray data on maps representing biological pathways and groupings of genes.

2.7. Reverse transcription (RT)-PCR

Semi-quantitative RT-PCR was performed as previously described (Chung et al., 2005a) with the primers listed in Table 1.

3. Results

3.1. Establishment of injury and regeneration stages

The histopathological evaluation of the livers of the animals treated with high doses of GalN showed spotty necrosis of hepatocytes and lymphocytic infiltration at 6 h, ballooning degeneration and hepatocellular necrosis with lymphocytic infiltration at 24 h, and recovery at 72 h after drug administration (Fig. 1). Upon low dose treatment, no histologic change was seen at 6, 24, and 72 h. Likewise, no histologic change was seen in vehicle-treated animals. Due to such mild injury to the liver, borderline changes were detected in serum transferase activities (data not shown). Based on such histopathologic and biochemical evaluation, we classified the GalN effect on mice liver into injury (6 and 24 h) and regeneration (72 h) stages.

3.2. Microarray analysis of GalN effect on gene expression

Whole microarray data could be found on the web at www.snubi.org/publication/TGRC_GALN. To verify the accuracy of the microarray assays, 10 genes were randomly chosen out of statistically reliable clones identified by two-way ANOVA (see below; Supplementary Table 1 at www.snubi.org/publication/TGRC_GALN), and semi-quantitative RT-PCR was performed with primers listed in Table 1. Most of the semi-quantitative

RT-PCR results are in reasonable agreement with the microarray results, when the concordance was provided by the percentage of genes that showed expression ratios in the same direction (i.e. either up- or down-regulation). When the RT-PCR results of six drug-treated conditions (two doses at three time points) were compared to that of non-treated for each individual gene by the direction of change of gene expression levels, 41 sets out of 60 (6 sets per gene, 10 genes total) showed concordant expression (68.3%; Fig. 2). The median of the three values (in $\log_2$ scale) for each condition was calculated, and the fold change versus the non-treated sample (NT) was defined as the expression level. Upon two-way ANOVA, a total of 7267 out of 33,315 (21.8%) gene probes were found to be statistically reliable at $p < 0.05$ (Supplementary Table 1 at www.snubi.org/publication/TGRC_GALN). Depending on the testing correction method, the numbers of statistically reliable clones were changed to 268, 2399, and 875 after Bonferoni correction, Benjamini–Hochberg correction
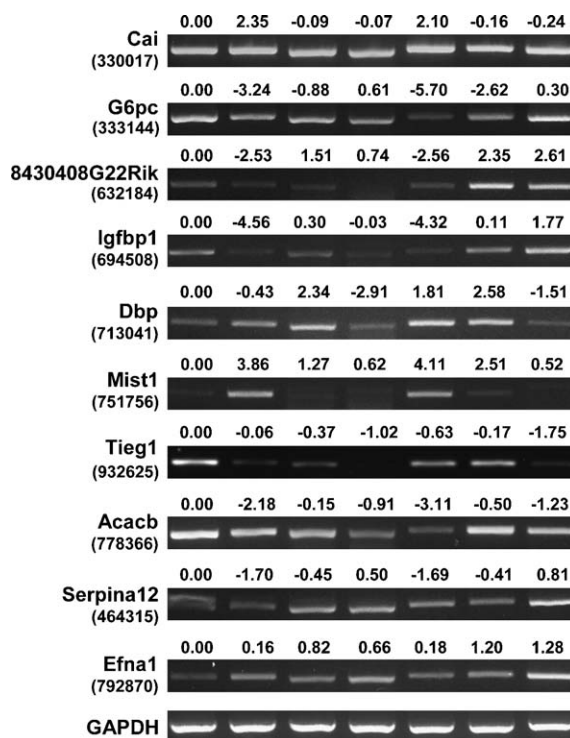

Fig. 2. Semi-quantitative RT-PCR and microarray results of selected clones. Fold changes in $\log_2$ scale from microarray analysis were illustrated above the semi-quantitative RT-PCR results. Each probe was presented by its gene symbol (left to the panel) and the corresponding Spot ID numbers were parenthesized. Numbers shown above the RT-PCR result were microarray data of the indicated Spot ID which were represented as fold change (in $\log_2$ value) vs. the non-treated control. From left to right: non-treated, low dose at 6 h, low dose at 24 h, low dose at 72 h, high dose at 6 h, high dose at 24 h, high dose at 72 h.
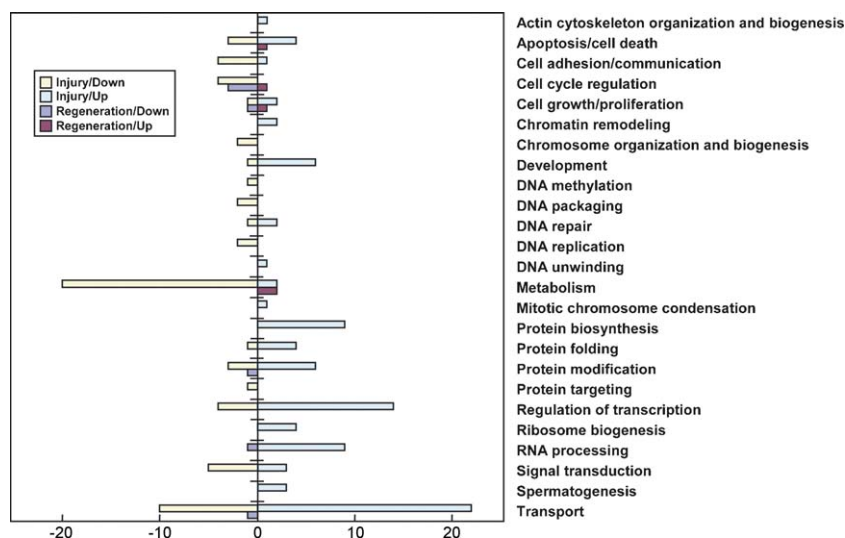
Fig. 3. Injury- and regeneration-specific genes classified by expression levels and gene function classified by GO. Genes with unknown functions were not presented.

and Benjamini–Yekutieli correction, respectively (Section 4.2 at www.snubi.org/publication/TGRC_GALN). The 7267 significant genes were further classified into eight groups under the terms of the saturated linear model as described in Section 2 (Supplementary Table 1 at www.snubi.org/publication/TGRC_GALN). Analysis of the transcriptomic data by two-way ANOVA showed 4240 of 7267 (58.3%) probes were below the value of 0.7 (in $\log_2$ scale) in all three vehicle-treated samples and above 0.7 in induction or suppression in at least one drug-treated condition (Supplementary Table 2 at www.snubi.org/publication/TGRC_GALN). Alternatively, when the whole data was statistically analyzed by a modified *t*-test analysis, SAM, against the non-treated control at FDR <5%, 1469 out of 33,315 (4.4%) probes were found to be statistically reliable (Supplementary Table 3 at www.snubi.org/publication/TGRC_GALN). By SAM, 460 of 1469 (31.3%) probes were below 0.7 in all three vehicle-treated samples and above 0.7 in induction or suppression in at least one drug-treated condition (Supplementary Table 4 at www.snubi.org/publication/TGRC_GALN). A comparison of the two lists of genes revealed 389 genes that were concordantly called "differentially regulated" by both analytical methods (Supplementary Table 5 at www.snubi.org/publication/TGRC_GALN). Throughout this study 0.7-fold was set as a threshold value.

3.3. Injury- and recovery-specific genes

As mentioned previously, acute GalN effect was classified into two stages of injury and regeneration.

Differentially regulated genes were further analyzed to identify injury- and regeneration-specific genes as previously described (Chung et al., 2006). Among the 389 differentially regulated genes selected by both analytical methods, 336 genes (Supplementary Tables 6 and 7 at www.snubi.org/publication/TGRC_GALN) and 13 genes (Supplementary Table 8 at www.snubi.org/publication/TGRC_GALN) were identified as injury- and regeneration-specific genes, respectively. These results show that more transcriptomic changes occurred during the injury stage than recovery stage. The differentially expressed genes were individually annotated with the GO terms (www.geneontology.org), classified by function, and plotted as injury- (336 clones) versus regeneration-specific clones (13 clones) and down- (146 clones) versus up-regulated clones (203 clones) (Fig. 3). Furthermore, these genes were also classified by GenMAPP analysis (Supplementary Table 9 at www.snubi.org/publication/TGRC_GALN). Intriguingly, some genes were classified into different functional categories by GO and GenMAPP analyses, due to multiple functions for a single gene.

4. Discussion

4.1. Genes associated with protein synthesis and degradation

GalN at doses high enough to induce acute hepatitis is known to involve inhibition of hepatic protein synthesis (Koff et al., 1971). Such protein synthesis inhibition is mediated by hexosamine-containing glycogen (amino-

Table 2
Differentially regulated genes by both GalN and diclofenac intoxication

Spot ID	Gene	GenBank	Function	D-Galactosamine						Diclofenac					
				L_6h[a]	L_24h	L_72h	H_6h	H_24h	H_72h	L_6h	L_24h	L_72h	H_6h	H_24h	H_72h
925122	1110017C15Rik	NM_025391	Ribosome biogenesis	0.70	−0.08	0.42	1.28	0.36	0.06	0.72	0.31	0.04	0.70	0.50	0.09
370565	4930402E16Rik	NM_198308	Carbohydrate metabolism	−0.27	0.32	0.42	−1.08	−0.05	0.43	0.26	−0.28	0.40	0.05	−0.73	0.32
907987	Acyp1	NM_025421	Carbohydrate metabolism	−0.62	−0.31	−0.27	−1.39	−0.16	−0.22	−0.46	−0.18	0.02	−0.94	−0.41	−0.32
470378	Akap8	NM_019774	Mitotic chromosome condensation	0.61	0.01	0.56	1.20	0.08	−0.23	0.91	−0.08	−0.25	0.47	0.09	0.07
918040	Atf5	NM_030693	Regulation of transcription	0.69	0.24	0.31	1.06	0.10	0.27	0.71	0.02	−0.05	0.95	−0.10	0.19
482840	BC027342	NM_146251	Ribosomal protein	−1.02	−0.43	−0.14	−1.73	−0.06	−0.17	−1.24	−0.06	0.24	−1.35	0.13	−0.10
468161	Eif2b4	NM_010122	Protein biosynthesis	0.57	−0.16	−0.14	1.10	−0.02	−0.31	0.77	−0.04	−0.41	0.65	0.09	−0.55
731749	Eif4b	NM_145625	Protein biosynthesis	0.24	−0.24	0.43	1.12	−0.19	0.39	−0.37	0.16	0.88	0.09	−0.22	0.58
901519	Hmgn1	NM_008251	DNA packaging	−0.79	−0.11	−0.26	−1.33	−0.14	−0.34	−0.47	−0.07	−0.37	−0.72	−0.10	−0.33
840369	Mgat2	NM_146035	Lipid metabolism	0.76	0.38	−0.14	0.95	0.07	−0.39	0.84	0.44	−0.23	0.80	0.04	−0.15
905986	Mrps28	NM_025434	mRNA processing	−0.90	−0.13	−0.44	−0.92	−0.06	−0.60	−0.87	−0.27	−0.57	−0.82	0.04	−0.54
477349	Pdgfa	NM_008808	Cell proliferation	−0.08	0.28	−0.52	1.32	0.38	−0.67	−0.04	0.29	−0.70	−0.05	−0.16	−0.59
634272	Pelo	NM_134058	Protein biosynthesis	0.90	0.52	0.51	1.43	0.31	−0.08	1.02	0.18	−0.37	0.71	0.13	0.00
694902	Ppp2r5e	NM_012024	Signal transduction	0.70	0.46	0.22	1.13	0.44	0.37	1.04	0.49	0.36	0.85	0.50	0.44
494716	Psen2	NM_011183	Signal transduction	−0.65	−0.74	−0.35	−1.55	−0.69	−0.57	−0.76	0.19	−0.20	−0.62	−0.17	−0.13
604826	Rbl2	NM_011250	Cell cycle regulation	−0.63	−0.61	−0.01	−1.59	−0.36	0.03	−0.85	−0.04	0.51	−0.71	−0.46	0.02
911591	Sfrs2	NM_011358	RNA processing	0.94	0.36	0.28	1.70	0.31	0.36	−0.85	−0.04	0.51	−0.71	−0.46	0.02
791646	Vegfb	NM_011697	Cell cycle regulation	−1.14	0.24	−0.19	−1.15	−0.32	−0.08	−1.11	0.26	0.24	−1.01	−0.10	0.30
777713	Wars	NM_011710	Protein biosynthesis	1.15	−0.02	−0.56	1.59	0.10	−0.48	0.00	0.08	−0.44	0.95	0.21	−0.13

Each value represents the fold change (in log$_2$ value) vs. the non-treated control.

[a] L_6, low dose at 6 h vs. non-treated; L_24, low dose at 24 h vs. non-treated; L_72, low dose at 72 h vs. non-treated; H_6, high dose at 6 h vs. non-treated; H_24, high dose at 24 h vs. non-treated; H_72, high dose at 72 h vs. non-treated.

glycogen), which could be reversed by epinephrine and glucagons (Meszaros et al., 1976; Mandl et al., 1982), and total protein per wet weight of liver is reported to be significantly reduced by GalN injury (Ferencikova et al., 2003). Intriguingly, protein synthesis is also important in the pathogenesis of GalN-induced hepatotoxicity, as pretreatment with protein synthesis inhibitor cycloheximide significantly protects intoxicated rats from fatality (Koff and Connelly, 1976). Upon microarray analysis, we observed differential expression of genes involved in protein translation (Supplementary Table 9 at www.snubi.org/publication/TGRC_GALN). Notably, several translational initiation factors were induced at 6 h with high dose of GalN: Eif2b4 (Spot ID 468161, Accession No. NM010122), Eif3s1 (Spot ID 391780, Accession No. NM144545), Eif3s10 (Spot ID 305716, Accession No. NM010123), Eif4b (Spot ID 731749, Accession No. NM145625). Intriguingly, Eif2b4 and Eif4b were among the 19 genes identified as common differentially regulated genes by both GalN and diclofenac intoxication (Table 2) (Chung et al., 2006). In addition, ribosomal proteins Rpl41 (Spot ID 467882, Accession No. NM018860) and Rpl21 (Spot ID 482840, Accession No. NM146251) were induced and reduced, respectively, at 6 h with both low and high doses. Although the number of ribosomal proteins genes affected were limited to only two genes, it is noteworthy because significant number of ribosomal protein genes has been reported to be differentially expressed by fatty liver-inducing carbon tetrachloride in rats (Chung et al., 2005a). Furthermore, differential expression was observed with genes involved in proteasome degradation: Ube2g2 (Spot ID 557486, Accession No. NM019803) was induced at 6 h, while Psmb10 (Spot ID 925595, Accession No. NM013640), H2afz (Spot ID 903349, Accession No. NM016750), Psmb9 (Spot ID 675630, Accession No. D44458) were downregulated at 6 h. Such gene expression changes may result in more protein synthesis and less protein degradation, which may act as a compensatory mechanism for the inhibition of protein synthesis caused by GalN.

4.2. Genes associated with mRNA processing and binding

Trapping of uracil nucleotides by GalN metabolites gives decreased synthesis of RNA due to deficiency of UTP (Decker et al., 1973). Many genes associated with mRNA processing and binding were identified as injury-specific genes by microarray analysis (Supplementary Table 9 at www.snubi.org/publication/TGRC_GALN). Sfrs2 (Spot ID 911591, Accession No. NM011358), which is a serine/arginine-rich protein (SR) comprising

the mRNA spliceosomal complex E, and a SR protein kinase Prpf4b (Spot ID 616195, Accession No. NM013830) were upregulated at 6 h by GalN. In addition, many genes encoding RNA binding proteins were classified as injury-specific genes. Mrps28 (Spot ID 905986, Accession No. NM025434), which is a mitochondrial ribosomal protein, was down-regulated at 6 h by GalN. Genes for cytoplasmic RNA binding proteins, Syncrip (Spot ID 597092, Accession No. NM019666), Pabpc4 (Spot ID 4896685, Accession No. NM130881), and Srp68 (Spot ID 307231, Accession No. NM146032), were upregulated during injury stage by GalN. Transcripts of nuclear RNA binding proteins Ncl (Spot ID 907017, Accession No. NM010880) and Ddx5 (Spot ID 904995, Accession No. NM007840) were augmented at 6 h by GalN. Intriguingly, mRNA expression of Htf9c (Spot ID 689104, Accession No. NM008307) was induced, whose encoded product possesses a tRNA(uracil-5-)-methyltransferase activity implied in tRNA maturation (Guarguaglini et al., 1997). In addition, Excosc4 (Spot ID 367465, Accession No. NM175399) gene, which encodes a protein with rRNA processing activity (Brouwer et al., 2001), was identified as a injury-specific gene. Such co-regulation of RNA processing and binding proteins are notable as GalN effect on RNA processing is largely unknown except for the net hypomethylation of rRNA by GalN (Clawson et al., 1990).

4.3. Genes associated with cell cycle regulation

Liver regeneration, an example of tissue recovery after injury, is induced by damage to liver structure and function. Interleukin-6 (IL-6) is reported as an important signal which enhances the survival of intoxicated animals with by preventing the progression of liver necrosis and is involved in initiating liver regeneration (Galun et al., 2000; Hecht et al., 2001; Ferencikova et al., 2003). However, IL-6 (Spot ID 924312, Accession No. NM031168) gene expression in the intoxicated liver was not changeable by GalN, suggesting the endocrine rather than autocrine origin of this cytokine. Liver regeneration upon GalN injury is also known to involve proliferation of both progenitor cell and hepatocytes. Progenitor cells are activated by GalN treatment to proliferate and differentiate into mature hepatocytes (Dabeva and Shafritz, 1993). In addition, hepatocytes proliferate to restore the liver mass after GalN liver injury, which is evidence by increased 5-bromo-2′-deoxyuridine (BrdU) incorporation (Dabeva and Shafritz, 1993; Kitten and Ferry, 1998; Asaoka et al., 2005). Intriguingly, several genes involved in cell cycle

progression were identified as injury-specific down-regulated genes by microarray analysis (Supplementary Table 9 at www.snubi.org/publication/TGRC_GALN): Cyclin A2 (Ccna2, Spot ID 643994, Accession No. NM009828), Cadherin 1 (Cdh1, Spot ID 925329, Accession No. NM009864), Atm (Spot ID 373292, Accession No. NM007499), and Prim2 (Spot ID 905997, Accession No. NM008922). Such changes in gene expression imply damage response to GalN during the injury stage, rather than induction of cell proliferation during regeneration.

In summary, we report the full chronological gene expression profile of mouse liver upon GalN administration by histopathology and microarray analyses. In particular, the GalN effect was divided into injury and regeneration stages despite very low doses of the intoxicant, and genes specific to each stage were discussed in association with functional categories. Many genes associated with protein synthesis and degradation, mRNA processing and binding, and cell cycle regulation yielded differential expression throughout the time course and doses investigated. We believe that our results would be valuable in not only understanding the mechanism of GalN-induced liver injury and subsequent recovery, but also for future application such as building a hepatotoxin toxochip.

Acknowledgements

References

Asaoka, Y., Sakai, H., Takahashi, N., Hirata, A., Tsukamoto, T., Yamamoto, M., Yanai, T., Masegi, T., Tatematsu, M., 2005. Intraperitoneal injection of D-galactosamine provides a potent cell proliferation stimulus for the detection of initiation activities of chemicals in rat liver. J. Appl. Toxicol. 25 (6), 554–561.

Bolstad, B.M., Irizarry, R.A., Astrand, M., Speed, T.P., 2003. A comparison of normalization methods for high density oligonucleotide array data based on variance and bias. Bioinformatics 19 (2), 185–193.

Brouwer, R., Allmang, C., Raijmakers, R., van Aarssen, Y., Egberts, W.V., Petfalski, E., van Venrooij, W.J., Tollervey, D., Pruijn, G.J., 2001. Three novel components of the human exosome. J. Biol. Chem. 276 (9), 6177–6184.

Chung, H., Hong, D.-P., Jung, J.-Y., Kim, H.-J., Jang, K.-S., Sheen, Y.-Y., Ahn, J.-I., Lee, Y.-S., Kong, G., 2005a. Comprehensive analysis of differential gene expression profiles on carbon tetrachloride-induced rat liver injury and regeneration. Toxicol. Appl. Pharmacol. 206 (1), 27–42.

Chung, H., Kim, H.-J., Jang, K.-S., Kim, M., Yang, J., Kim, J.H., Lee, Y.-S., Kong, G., 2006. Comprehensive analysis of differential gene expression profiles on diclofenac-induced acute mouse liver injury and recovery. Toxicol. Lett. doi:10.1016/j.toxlet.2006.05.016.

Chung, H.J., Kim, M., Park, C.H., Kim, J., Kim, J.H., 2004. ArrayX-Path: mapping and visualizing microarray gene-expression data with integrated biological pathway resources using Scalable Vector Graphics. Nucleic Acids Res. 32 (Web Server issue), W460–W464.

Chung, H.J., Park, C.H., Han, M.R., Lee, S., Ohn, J.H., Kim, J., Kim, J.H., 2005b. ArrayXPath II: mapping and visualizing microarray gene-expression data with biomedical ontologies and integrated biological pathway resources using Scalable Vector Graphics. Nucleic Acids Res 33 (Web Server issue), W621–W626.

Clawson, G.A., Sesno, J., Milam, K., Wang, Y.F., Gabriel, C., 1990. The hepatocyte protein synthesis defect induced by galactosamine involves hypomethylation of ribosomal RNA. Hepatology 11 (3), 428–434.

Dabeva, M.D., Shafritz, D.A., 1993. Activation, proliferation, and differentiation of progenitor cells into hepatocytes in the D-galactosamine model of liver regeneration. Am. J. Pathol. 143 (6), 1606–1620.

Decker, K., Keppler, D., Pausch, J., 1973. The regulation of pyrimidine nucleotide level and its role in experimental hepatitis. Adv. Enzyme Regul. 11, 205–230.

Fausto, N., 2000. Liver regeneration. J. Hepatol. 32 (1 Suppl), 19–31.

Ferencikova, R., Cervinkova, Z., Drahota, Z., 2003. Hepatotoxic effect of D-galactosamine and protective role of lipid emulsion. Physiol. Res. 52 (1), 73–78.

Galun, E., Zeira, E., Pappo, O., Peters, M., Rose-John, S., 2000. Liver regeneration induced by a designer human IL-6/sIL-6R fusion protein reverses severe hepatocellular injury. FASEB J. 14 (13), 1979–1987.

Guarguaglini, G., Battistoni, A., Pittoggi, C., Di Matteo, G., Di Fiore, B., Lavia, P., 1997. Expression of the murine RanBP1 and Htf9-c genes is regulated from a shared bidirectional promoter during cell cycle progression. Biochem. J. 325 (Pt 1), 277–286.

Hecht, N., Pappo, O., Shouval, D., Rose-John, S., Galun, E., Axelrod, J.H., 2001. Hyper-IL-6 gene therapy reverses fulminant hepatic failure. Mol. Ther. 3 (5 Pt 1), 683–687.

Ihaka, R., Gentleman, R., 1996. R: a language for data analysis and graphics. J. Comput. Graphical Stat. 5 (3), 299–314.

Isozaki, M., Masubuchi, Y., Horie, T., 2002. Evaluation of drug-induced hepatotoxicity by plasma retinol binding protein. In Vivo 16 (1), 61–65.

Keppler, D., Lesch, R., Reutter, W., Decker, K., 1968. Experimental hepatitis induced by D-galactosamine. Exp. Mol. Pathol. 9 (2), 279–290.

Kinoshita, T., Tashiro, K., Nakamura, T., 1989. Marked increase of HGF mRNA in non-parenchymal liver cells of rats treated with hepatotoxins. Biochem. Biophys. Res. Commun. 165 (3), 1229–1234.

Kitten, O., Ferry, N., 1998. Mature hepatocytes actively divide and express gamma-glutamyl transpeptidase after D-galactosamine liver injury. Liver 18 (6), 398–404.

Koff, R.S., Connelly, L.J., 1976. Modification of the hepatotoxicity of D-galactosamine in the rat by cycloheximide. Proc. Soc. Exp. Biol. Med. 151 (3), 519–522.

Koff, R.S., Fitts, J.J., Sabesin, S.M., Zimmerman, H.J., 1971. D-Galactosamine hepatotoxicity. II. Mechanism of fatty liver production. Proc. Soc. Exp. Biol. Med. 138 (1), 89–92.

Lozano, J.M., Padillo, J., Montero, J.L., Pena, J., De la Mata, M., Muntane, J., 2003. Immunomodulatory activity of TNF-alpha during acute liver injury induced by D-galactosamine and its protection by PGE1 in rats. Int. Immunopharmacol. 3 (2), 197–207.

Mandl, J., Meszaros, K., Antoni, F., Spolarics, Z., Garzo, T., 1982. Reversible inhibition of RNA synthesis and irreversible inhibition of protein synthesis by D-galactosamine in isolated mouse hepatocytes. Mol. Cell. Biochem. 46 (1), 25–30.

Meszaros, K., Mandl, J., Antoni, F., Garzo, T., 1976. Inhibition of protein synthesis by hexosamine containing glycogen formed in mouse liver after treatment with D-galactosamine. FEBS Lett. 71 (2), 215–219.

Muntane, J., Montero, J.L., Marchal, T., Perez-Seoane, C., Lozano, J.M., Fraga, E., Pintado, C.O., de la, M., Mino, G., 1998. Effect of PGE1 on TNF-alpha status and hepatic D-galactosamine-induced apoptosis in rats. J. Gastroenterol. Hepatol. 13 (2), 197–207.

Nuwaysir, E.F., Bittner, M., Trent, J., Barrett, J.C., Afshari, C.A., 1999. Microarrays and toxicology: the advent of toxicogenomics. Mol. Carcinog. 24 (3), 153–159.

Plaa, G.L., 1991. Toxic response of the liver. In: Amdur, M.O., Doull, J., Klaassen, C.D. (Eds.), Casarett and Doull's Toxicology. Permagon Press, New York, pp. 334–353.

Reitman, S., Frankel, S., 1957. A colorimetric method for the determination of serum glutamic oxalacetic and glutamic pyruvic transaminases. Am J Clin Pathol 28 (1), 56–63.

Schena, M., Shalon, D., Davis, R.W., Brown, P.O., 1995. Quantitative monitoring of gene expression patterns with a complementary DNA microarray. Science 270 (5235), 467–470.

Sun, F., Hamagawa, E., Tsutsui, C., Sakaguchi, N., Kakuta, Y., Tokumaru, S., Kojo, S., 2003. Evaluation of oxidative stress during apoptosis and necrosis caused by D-galactosamine in rat liver. Biochem. Pharmacol. 65 (1), 101–107.

Troyanskaya, O., Cantor, M., Sherlock, G., Brown, P., Hastie, T., Tibshirani, R., Botstein, D., Altman, R.B., 2001. Missing value estimation methods for DNA microarrays. Bioinformatics 17 (6), 520–525.

Tsutsui, S., Hirasawa, K., Takeda, M., Itagaki, S., Kawamura, S., Maeda, K., Mikami, T., Doi, K., 1997. Apoptosis of murine hepatocytes induced by high doses of galactosamine. J. Vet. Med. Sci. 59 (9), 785–790.

Yata, Y., Takahara, T., Furui, K., Zhang, L.P., Watanabe, A., 1999. Expression of matrix metalloproteinase-13 and tissue inhibitor of metalloproteinase-1 in acute liver injury. J. Hepatol. 30 (3), 419–424.